ELSEVIER

Surface Science 491 (2001) 239–254

SURFACE SCIENCE

www.elsevier.com/locate/susc

Self-consistent rate-equation approach to irreversible submonolayer growth in one dimension

Jacques G. Amar [a,*], Mihail N. Popescu [b], Fereydoon Family [b]

[a] *Department of Physics and Astronomy, University of Toledo, Toledo, OH 43606, USA*
[b] *Department of Physics, Emory University, Atlanta, GA 30322, USA*

Received 16 March 2001; accepted for publication 29 June 2001

Abstract

A self-consistent rate-equation (RE) approach to irreversible submonolayer growth in one dimension is presented. Our approach is based on a set of dynamical equations for the evolution of gaps between islands which is coupled to the island-density REs via local capture numbers and explicitly takes into account correlations between the size of an island and the corresponding capture zone. In the most simple formulation, fragmentation of capture zones is not directly included, but accounted for through a uniform rescaling, while nucleation is assumed to generate only gaps with average length. Using this approach, we have been able to accurately predict the scaled island-size, capture-number, and average-gap-size distributions in the pre-coalescence regime. Our approach also leads to a novel analytical expression for the monomer capture number $\sigma_1 = (4/RN_1\gamma)^{1/2}$ where N_1 is the monomer density, γ is the fraction of the substrate covered by islands, and R is the ratio D/F of the diffusion rate to deposition flux which agrees with simulations over the entire pre-coalescence regime, and implies a novel scaling behavior for the island density at low coverage, in contrast to earlier predictions. Comparisons between our RE results and kinetic Monte Carlo simulations are presented for both point islands and extended islands. © 2001 Published by Elsevier Science B.V.

Keywords: Molecular beam epitaxy; Growth; Nucleation; Models of surface kinetics; Monte Carlo simulations; Non-equilibrium thermodynamics and statistical mechanics; Vicinal single crystal surfaces

1. Introduction

Molecular beam epitaxy (MBE) offers the possibility of atomic-scale controlled production of thin films, high quality crystals, and nanostructures. The dominant processes in the early stages of growth involve nucleation, aggregation and coalescence of islands. The resulting island density and size distributions play an important role in determining the quality of the multilayer growth or of the desired nanostructures.

The recent development of experimental methods such as scanning tunneling microscopy (STM) and reflection high energy electron diffraction (RHEED) has made possible the real-time probing of the surface evolution during the early stages of thin-film growth [1]. This has led to a renewed experimental interest in understanding and characterizing epitaxial growth [2–16] and has also stimulated considerable theoretical work toward a better understanding of the scaling properties of

* Corresponding author. Tel.: +1-419-530-2259; fax: +1-419-530-2723.
E-mail address: jamar@physics.utoledo.edu (J.G. Amar).

0039-6028/01/$ - see front matter © 2001 Published by Elsevier Science B.V.
PII: S0039-6028(01)01411-X

the island density and island-size distribution in submonolayer growth [17–41].

Although submonolayer growth is usually two dimensional, in some cases it can be effectively one dimensional. For example, during heterogeneous deposition on a cleaved surface, nucleation often occurs preferentially on steps rather than on the free surface, and in cases when monomer diffusion along the steps is also dominant this leads to quasi one-dimensional growth. The deposition of gold on stepped sodium chloride substrates has recently been studied by Gates and Robins [24–26]. The decoration of steps by clusters has also been used to study the behavior of surface steps, and recently it has been suggested that this offers the possibility of controlled growth of nanoclusters [36]. For systems with an extremely high anisotropy, such as the 2×1-row-reconstructed Si(0 0 1) surface [2] or the 2×1 reconstructed Pt(1 0 0) surface [37], it is also possible to have quasi one-dimensional growth [39].

One of the standard tools used in studying submonolayer growth is the rate-equation (RE) approach [42,43]. This approach involves a set of deterministic coupled reaction–diffusion equations describing the coverage dependence of average quantities through a set of rate coefficients usually called capture numbers [17–19,42,43]. As has been pointed out [17–19,29,31,35] one of the central problems in this approach is the determination of the magnitude and size dependence of the capture numbers.

Here we present a self-consistent RE approach to one-dimensional irreversible submonolayer growth in which the capture numbers are explicitly calculated by taking into account correlations between the size of an island and the corresponding capture zone. Using this approach, we first derive a novel analytical expression for the monomer–monomer capture number in one-dimensional irreversible growth. To obtain the island-size distribution, a second set of mean-field (MF) equations is used to describe the evolution of the island-size dependent capture zones, leading to explicit size- and coverage-dependent capture numbers. A numerical solution of the resulting set of REs leads to predictions for the size-dependent capture numbers and island-size distributions which agree well with simulations.

We note that in recent work [34] Blackman and Mulheran have pointed out the importance of fluctuations and have also developed a RE approach to one-dimensional irreversible growth. In their approach, the dependence of the average monomer and island capture numbers on the average monomer and island densities was expressed in terms of two phenomenological parameters whose values were determined by simulations. By using these parameters and assuming scaling, this approach was extended [36] to predict the island-size distribution in terms of the distribution of gaps between islands, which was determined by Monte Carlo simulations. In contrast, in our approach scaling is not assumed but is found to arise naturally from the solution of our gap-evolution and island-density REs. In addition, the distribution of average gap sizes is explicitly predicted in the course of the calculation.

2. Model and simulations

Fig. 1 shows schematically the physical processes involved during irreversible submonolayer growth. As can be seen these involve random deposition, diffusion, dimer nucleation, and island growth or aggregation of adatoms (monomers). Also shown in Fig. 1 is the "gap" y between a dimer and the nearest island to its right as well as the "capture zone" corresponding to the region between the midpoints of the gaps on each side.

In order to study the effects of island morphology on the island-size distribution in one-dimensional submonolayer growth, we have studied two different models – a point-island model and a more realistic extended-island model. As shown in Fig. 1, in both models atoms are deposited randomly on an initially empty line of M sites with a (per site) deposition rate F and may diffuse to nearest-neighbor sites with hopping rate D_h. In the point-island model (Fig. 1(a)) an island occupies a single site. When a monomer moves onto a site occupied by another monomer, a dimer island is nucleated at that site. Similarly, a monomer moving onto a site occupied by an island is absorbed and the island size s increases by one. In contrast, in the extended-island model (Fig. 1(b)) the islands are allowed to

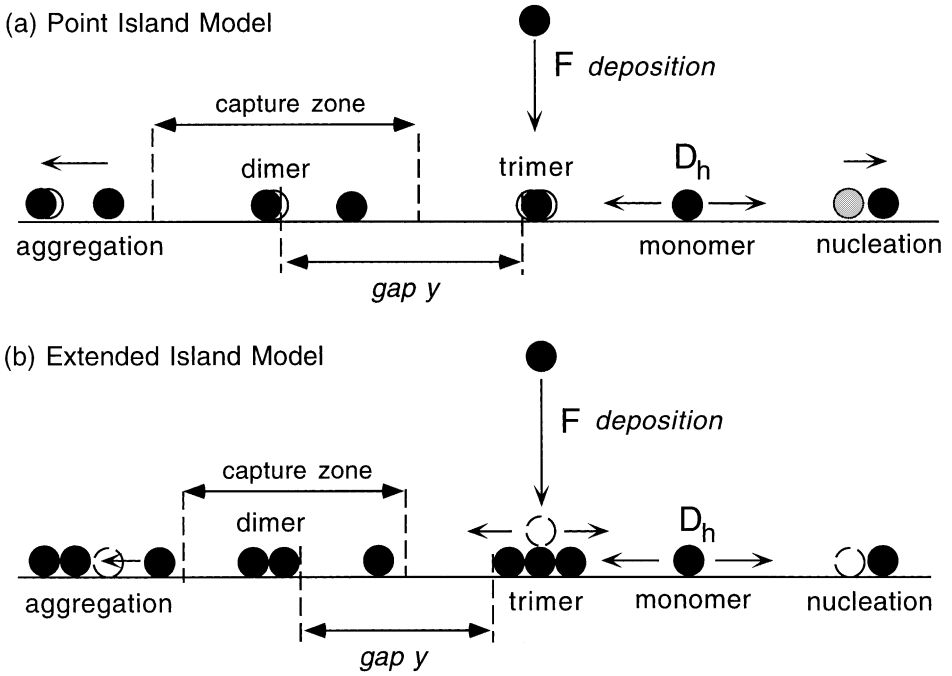

Fig. 1. Schematic diagram showing processes of diffusion, deposition, and aggregation for (a) point-island model and (b) extended-island model.

grow laterally by irreversible attachment of atoms at nearest-neighbor sites. Atoms with one or more nearest neighbors are assumed to be immobile while monomers landing on top of an island diffuse on the surface until they fall off an edge and are incorporated into the island. Monomers landing on another monomer are immediately incorporated into the first layer and nucleate a dimer.

In order to obtain good statistics for the average monomer and island densities and island-size distributions in our simulations, very large system sizes of $M = 5 \times 10^5$ and 10^6 were used and averages were taken over 30–100 runs. The ratio $R_h = D_h/F$ of the monomer hopping rate D_h to the deposition rate F was varied from 10^5 to 10^8.

3. Self-consistent rate equations for submonolayer growth

3.1. Mean-field rate equations

The RE approach [17–19,42,43] involves a set of deterministic coupled reaction-diffusion equations describing the time (coverage) dependence of the average densities of monomers, N_1, and of islands of size $s \geqslant 2$, N_s, where s is the number of atoms in the island. A general form of these equations, valid for irreversible growth in the pre-coalescence regime, may be written

$$\frac{dN_1}{d\theta} = \gamma - 2N_1 - 2R\sigma_1 N_1^2 - RN_1 \sum_{s \geqslant 2} \sigma_s N_s \qquad (1)$$

$$\frac{dN_s}{d\theta} = RN_1(\sigma_{s-1}N_{s-1} - \sigma_s N_s) + k_{s-1}N_{s-1} - k_s N_s \quad \text{for } s \geqslant 2 \qquad (2)$$

where $\theta = Ft$ is the coverage, and $R = D/F$ is the ratio of the monomer diffusion rate $D = D_h/2$ to the (per site) deposition rate F. In these equations, the terms with σ_s correspond to the capture of diffusing monomers by other monomers or by existing islands, while the terms with k_s (where $k_s = s$ for extended islands and $k_s = 1$ for point islands) correspond to the deposition of adatoms directly on islands of size s. The first two terms on the right

side of Eq. (1) correspond to the gain in monomers due to deposition flux minus the rate of loss due to direct impingement on existing monomers or islands. The quantity γ (where $\gamma = 1 - \theta + N_1$ for extended islands and $\gamma = 1 - N$ for point islands) corresponds to the fraction of the substrate which is not covered by islands.

Once the coverage-dependent capture numbers $\sigma_s(\theta)$ are known, then Eqs. (1) and (2) can be numerically solved to find the island densities $N_s(\theta)$ as a function of coverage. If we define the total island density $N = \sum_{s \geqslant 2} N_s$ and identify $2\sigma_1 N_1 = 1/\xi_1^2$ and $1/\xi^2 = 1/\xi_1^2 + \sum_{s \geqslant 2} \sigma_s N_s$, we may also obtain a simpler set of contracted REs for the total island density N and monomer density N_1,

$$\frac{dN_1}{d\theta} = \gamma - 2N_1 - RN_1/\xi^2 \tag{3}$$

$$\frac{dN}{d\theta} = RN_1/2\xi_1^2 + N_1 \tag{4}$$

These equations can be numerically integrated once the "nucleation length" ξ_1 and "monomer capture length" ξ are known.

3.2. Self-consistent equation for capture numbers σ_s

In order to carry out a self-consistent calculation of the capture numbers σ_s entering into the REs (1) and (2), we need to first calculate the microscopic capture rate of monomers near an island and then compare with the corresponding "capture" terms in the REs. In particular, we consider the following diffusion equation for the *local* monomer density $n_1(x,\theta)$ in a gap of length y between the edge of an island and the edge of the neighboring island,

$$\frac{\partial n_1}{\partial \theta} = 1 - 2n_1 + R\nabla^2 n_1 - Rn_1/\xi_1^2 \tag{5}$$

with boundary conditions appropriate for irreversible growth i.e. $n_1(0) = n_1(y) = 0$. The first two terms on the right side of Eq. (5) correspond to deposition minus direct impingement of monomers on monomers while the last two terms correspond to monomer diffusion and nucleation respectively. Multiplying Eq. (5) by γ and subtracting the contracted RE (3) one obtains

$$\nabla^2 n_1 - \xi_1^{-2}(n_1 - (\alpha^2/\gamma)N_1) = \frac{1}{\gamma R}\left(\gamma\frac{\partial n_1}{\partial \theta} - \frac{\partial N_1}{\partial \theta}\right) + \frac{2}{\gamma R}(\gamma n_1 - N_1) \tag{6}$$

where $\alpha^2 = \xi_1^2/\xi^2$. Since γ represents the fraction of sites that are not occupied by islands, the proper normalization of the monomer density is $\gamma\bar{n}_1 = N_1$ where $\bar{n}_1$ is the average local monomer density in all the gaps. Along with the factor of $1/R$, this implies that the right side of Eq. (6) may be neglected so that

$$\nabla^2 n_1 - \xi_1^{-2}(n_1 - (\alpha^2/\gamma)N_1) \simeq 0 \tag{7}$$

Using the boundary conditions $n_1(0) = n_1(y) = 0$, the solution is

$$n_1(x) = (\alpha^2 N_1/\gamma)\left(1 - \frac{\cosh[(x - y/2)/\xi_1]}{\cosh[y/(2\xi_1)]}\right) \tag{8}$$

Equating the RE-like expression $D\sigma_s N_1$ for the rate of capture of a monomer by an island of size s to the microscopic rate of capture $2D[dn_1/dx]_{x=0}$ (the factor of two comes from assuming that the gaps on both sides of the island are the same) leads to an expression for the "local" capture number $\tilde{\sigma}(y)$ corresponding to a gap of size y,

$$\tilde{\sigma}(y) = \frac{2\xi_1}{\gamma\xi^2}\tanh(y/(2\xi_1)) \tag{9}$$

We note that, in analogy with previous work [34,35] in which the importance of a Voronoi cell construction has been emphasized in describing the "capture zone" of an island in two dimensions, one may define the capture zone of an island as corresponding to the Voronoi region delimited by the bisectors of the gaps between islands as shown in Fig. 1. Here, however, we find it simpler to calculate the capture number $\tilde{\sigma}(y)$ directly in terms of the gap distance y to the nearest island, where we associate one gap (say the gap on the right) with each island. Averaging over the gap distribution $G_s(y)$, corresponding to the density of gaps of size y on the right of an island of size s, leads to the average capture number σ_s i.e.,

$$\sigma_s = \langle \tilde{\sigma}(y) \rangle_{G_s(y)} = \frac{\sum_y G_s(y)\tilde{\sigma}(y)}{\sum_y G_s(y)} = \frac{1}{N_s} \sum_y G_s(y)\tilde{\sigma}(y) \quad (10)$$

Once the monomer nucleation length ξ_1 and the distribution of gap sizes $G_s(y)$ are known, then the capture length ξ and the capture numbers σ_s may be calculated self-consistently using Eqs. (9) and (10) along with the "capture number self-consistency condition",

$$\sum_{s \geqslant 2} N_s \sigma_s + 1/\xi_1^2 = 1/\xi^2 \quad (11)$$

Defining the overall gap distribution $G(y) = \sum_{s \geqslant 2} G_s(y)$, this condition may be rewritten,

$$\sum_y G(y)\tilde{\sigma}(y) + 1/\xi_1^2 = 1/\xi^2 \quad (12)$$

It is worth noting that using the capture-number self-consistency condition (12) along with the "sum-rule" $\sum_y G(y)y = \gamma$, and Eq. (9) for the local capture number $\tilde{\sigma}(y)$ one may show that the monomer density $n_1(x)$ as given by Eq. (8) satisfies the monomer density self-consistency condition,

$$\bar{n}_1 \equiv (1/\gamma) \sum_y G(y) \int_0^y n_1(x)\mathrm{d}x = N_1/\gamma \quad (13)$$

where the factor of $(1/\gamma)$ in the middle expression is due to the fact that the gap distribution $G(y)$ is normalized to the total substrate length rather than to the total gap length.

3.3. Mean-field solution for ξ_1

To calculate the nucleation length ξ_1 we have used a MF approach similar to that used by Bales and Chrzan [29] for the case of deposition on a two-dimensional substrate. In this approach we replace the "capture" of monomers by other monomers and islands in the region "outside" a given monomer by an overall smeared "sink" term of the form Rn_1/ξ^2. The resulting diffusion equation for the monomer density $n_1(x)$ near the monomer is the same as Eq. (5) except that ξ_1 is now replaced by ξ. Multiplying this equation by γ and subtracting the contracted RE (3) one obtains

$$\nabla^2 n_1 - \xi^{-2}\left(n_1 - \frac{1}{\gamma}N_1\right) = \frac{1}{\gamma R}\left(\gamma\frac{\partial n_1}{\partial\theta} - \frac{\partial N_1}{\partial\theta}\right) + \frac{2}{\gamma R}(\gamma n_1 - N_1) \quad (14)$$

Since $\gamma\bar{n}_1 = N_1$, the righthand side is zero on average and one obtains,

$$\nabla^2 n_1 - \xi^{-2}\left(n_1 - \frac{1}{\gamma}N_1\right) = 0 \quad (15)$$

Just as before, the factor of $1/\gamma$ takes into account the fact that the average local monomer density in the gaps is actually larger than the *overall* monomer density by a factor of $1/\gamma$. Using the boundary conditions $n_1(0) = 0$ and $n_1(\infty) = N_1/\gamma$ the solution is

$$n_1(x) = \frac{N_1}{\gamma}(1 - \mathrm{e}^{-x/\xi}) \quad (16)$$

Equating the RE-like expression $2D\sigma_1 N_1$ for the (per monomer) rate of nucleation to the microscopic rate of capture of a monomer by another monomer $4D[\mathrm{d}n_1/\mathrm{d}x]_{x=0}$ (one factor of 2 comes from the two "sides" of a monomer while the extra factor of 2 comes from the fact that the "relative" diffusion rate of monomers with respect to other monomers is twice the monomer diffusion rate) gives

$$\sigma_1 = 2/(\xi\gamma) \quad (17)$$

Using the definition $2\sigma_1 N_1 = 1/\xi_1^2$ this implies the MF result,

$$\xi_1 = \left(\frac{\xi\gamma}{4N_1}\right)^{1/2} \quad (18)$$

From the contracted RE (3) for the monomer density, we know that at late-time $\mathrm{d}N_1/\mathrm{d}\theta = \gamma - RN_1/\xi^2 \simeq 0$ so that $\xi \simeq (RN_1/\gamma)^{1/2}$. Substituting into Eq. (18), we obtain the following analytic expression for the monomer nucleation length ξ_1,

$$\xi_1 = \frac{1}{2}\left(\frac{R\gamma}{N_1}\right)^{1/4} \quad (19)$$

Although derived using a "late-time" assumption, this expression for ξ_1 works extremely well in predicting the rate of nucleation of dimers from monomers at *all* times, including very early times. In contrast, the MF expression (18) only applies at late times after the nucleation regime. Using the relation $1/\xi_1^2 = 2\sigma_1 N_1$, Eq. (19) also implies the unusual result for the monomer capture number,

$$\sigma_1 = \left(\frac{4}{RN_1\gamma}\right)^{1/2} \tag{20}$$

which indicates that in one dimension the monomer capture number σ_1 depends strongly on the monomer density N_1.

In order to test these results, we have measured the quantity $1/\xi_1^2 = 2\sigma_1 N_1$ as a function of coverage using kinetic Monte Carlo (KMC) simulations for both point islands and extended islands and compared with theoretical predictions. Simulations were carried out over a range of values of $R_h = D_h/F$ ranging from 10^5 to 10^8. The Monte Carlo simulation results for $1/\xi_1^2$ were calculated by measuring the nucleation rate $dN/d\theta$ and then using the expression (see Eq. (4)) $1/\xi_1^2 = (2/(RN_1))[(dN/d\theta) - N_1]$, while the theoretical results were obtained using Eq. (20) along with the monomer density N_1 obtained from simulation. As can be seen in Fig. 2, for both point and extended islands there is good agreement over all coverages in the pre-coalescence regime.

In the low-coverage "nucleation" regime for which $N \ll N_1$ and $N_1 \simeq \theta$, Eq. (20) implies that

$$N \simeq (4/5)R^{1/2}\theta^{5/2} \tag{21}$$

As can be seen in Fig. 3, simulation results for the island density N at low coverage are in excellent agreement with Eq. (21). If we define θ_x as the coverage corresponding to the crossover from the "early-time" nucleation regime when $N \ll N_1$ to the aggregation regime when $N \gg N_1$, such that $N(\theta_x) \simeq N_1 \simeq \theta_x$, then Eq. (21) implies that

$$\theta_x = (5/4)^{2/3}R^{-1/3} \tag{22}$$

for the case of one-dimensional irreversible submonolayer growth.

It is interesting to compare our theoretical predictions (9) and (20) for the local capture number

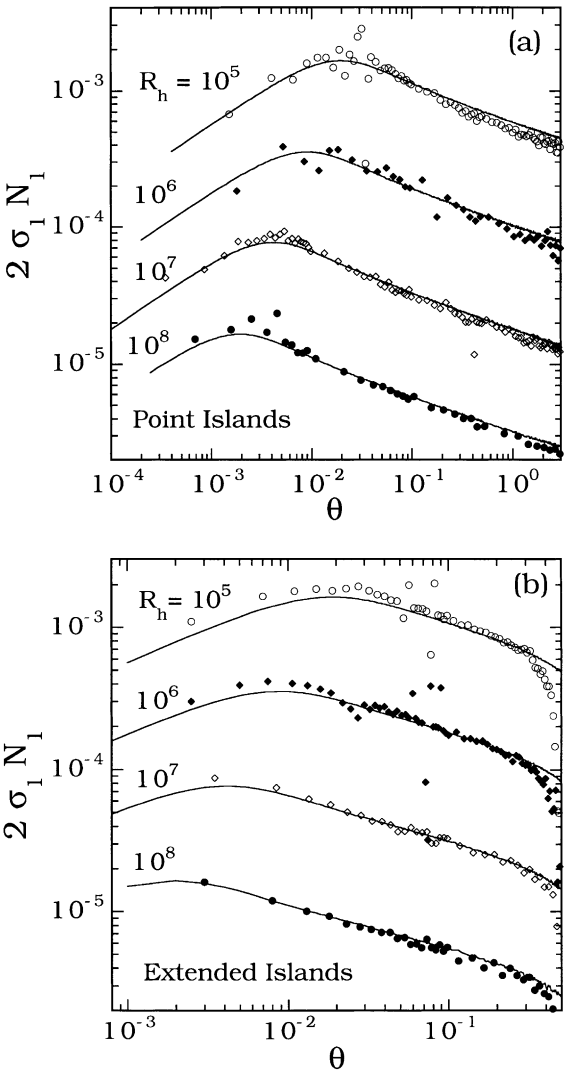

Fig. 2. Comparison of scaled nucleation rate $2\sigma_1 N_1$ calculated using Eq. (20) (solid lines) as a function of coverage θ for $D_h/F = 10^5$–10^8 with KMC simulation results (symbols) for (a) point islands and (b) extended islands.

$\tilde{\sigma}(y)$ and the monomer capture number σ_1 with the corresponding one-dimensional scaling predictions [34] $\sigma_1 \sim \sigma_{av} \sim N$ for $\theta \gg \theta_x$ and $\sigma_1 \sim \sigma_{av} \sim N_1$ for $\theta \ll \theta_x$ which may also be obtained using random walk arguments [19]. For $\theta \gg \theta_x$, the monomer density N_1 is small and $N_1 \ll N$ which implies that $\xi_1 \gg \xi$ while the monomer capture length ξ is of the order of the average gap size i.e. $\xi \sim \langle y \rangle \sim \gamma/N$.

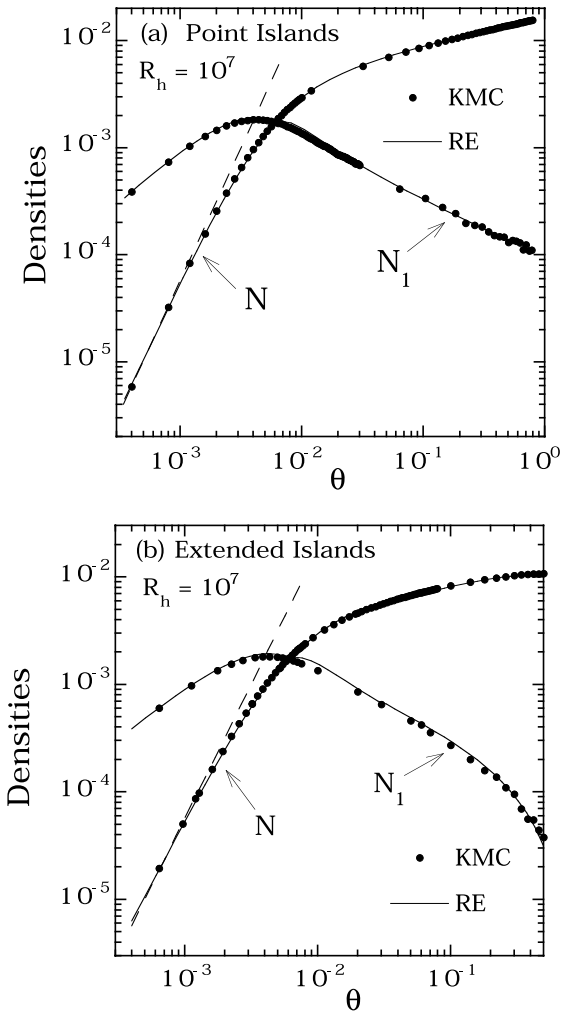

Fig. 3. Island and monomer densities N and N_1 as a function of coverage θ for $D_h/F = 10^7$ obtained using contracted REs (3) and (4) along with Eqs. (19) and (29) (solid lines) along with corresponding KMC results (symbols) for (a) point islands and (b) extended islands. Dashed lines correspond to Eq. (21).

Eq. (9) then implies $\sigma_{av} \simeq \sigma(\xi) \sim N$ in agreement with the random walk prediction. Similarly, for $\theta \gg \theta_x$, one has as before, $RN_1/\xi^2 = \gamma$ and Eq. (20) implies that $\sigma_1 \sim 1/\xi \sim N$ which is also in agreement with the random walk prediction. Thus, our results agree with the scaling behavior predicted by the random-walk analysis for $\theta \gg \theta_x$. Furthermore, using the relation $\xi \simeq (RN_1/\gamma)^{1/2}$ (valid at late-time) one may show that for $\theta \gg \theta_x$ the expression for σ_1 given in Ref. [34] is equivalent to Eq. (20). For $\theta \ll \theta_x$, one has $\xi_1 \simeq \xi \sim 1/N_1$ and $\langle y \rangle \sim 1/N \gg \xi_1$, so that Eq. (9) implies $\sigma_{av} \simeq \sigma(\langle y \rangle) \sim N_1$ which is also in agreement with the random-walk prediction. However, as indicated by Eqs. (20) and (21) and confirmed in Fig. 3, for $\theta \ll \theta_x$, one has $\sigma_1 = 2/\sqrt{RN_1}$ which implies $N = (4/5)R^{1/2}\theta^{5/2}$. The latter result is in strong contrast to the prediction $N = 2R\theta^4$ for $\theta \ll \theta_x$ obtained using σ_1 from Ref. [34]. Thus Eqs. (19) and (20) provide simple accurate analytical expressions for ξ_1 and σ_1 including all relevant prefactors, which are valid at all coverages in the pre-coalescence regime.

3.4. Fluctuations in one dimension

Using Eq. (9) for $\tilde{\sigma}(y)$ along with the sum rule $\sum_y G(y) = N$, the capture number self-consistency condition (12) may be rewritten

$$1/\xi^2 = 1/\xi_1^2 + (2N\xi_1/\gamma\xi^2)\langle \tanh(y/2\xi_1)\rangle_{G(y)} \qquad (23)$$

where the brackets denote an average over the gap distribution $G(y)$ i.e. $\langle f(y)\rangle_{G(y)} = (1/N)\sum_y f(y)\, G(y)$. Solving for ξ we obtain

$$\xi^2 = \xi_1^2[1 - (2N\xi_1/\gamma)\langle \tanh(y/2\xi_1)\rangle_{G(y)}] \qquad (24)$$

Replacing y by the average gap length $\langle y \rangle = \gamma/N$ leads to the MF prediction,

$$\xi^2 = \xi_1^2[1 - (2N\xi_1/\gamma)\tanh(\gamma/(2N\xi_1))] \qquad (25)$$

For $\theta \gg \theta_x$, the monomer density is low so that $N\xi_1 \gg 1$ and one may expand $\tanh(z) \simeq z - z^3/3$ to obtain

$$\xi^2 \simeq \gamma^2/(12N^2) \qquad (26)$$

However, due to the existence of large fluctuations in one dimension, this result is not correct. Instead one must average over the distribution of gap sizes y in order to self-consistently find the "capture length" ξ. While in general we need to know the gap distribution $G(y)$, at late times we can again expand the $\tanh(z)$ in Eq. (24) to obtain

$$\xi^2 = \langle Y^3\rangle\gamma^2/(12N^2) \qquad (27)$$

in agreement with Ref. [34] where $Y = y/\langle y \rangle$ and $\langle y \rangle = \gamma/N$. From KMC simulations we find $\langle Y^3 \rangle \simeq 1.6$ (see also Ref. [34]) for $\theta \gg \theta_x$ for both

point and extended islands. This implies that for $\theta \gg \theta_x$ the MF prediction (26) must be multiplied by a factor of $\langle Y^3 \rangle \simeq 1.6$ to take into account fluctuations in the gap distribution. Including this correction leads to the following corrected equation for the monomer capture length,

$$\xi^2 = \langle Y^3 \rangle \xi_1^2 [1 - (2N\xi_1/\gamma)\tanh(\gamma/(2N\xi_1))] \qquad (28)$$

where $\langle Y^3 \rangle \simeq 1.6$ for $\theta \gg \theta_x$ and $\langle Y^3 \rangle \simeq 1$ for $\theta \ll \theta_x$. We note that in order to ensure a "gradual" transition in the correction factor for ξ^2 (from 1.0 at early time to 1.6 at late time) a slight modification of Eq. (28) may be made. This leads to the following equation for the monomer capture length,

$$\xi^2 = \xi_1^2 \Big[1 - \Big(2N\xi_1 / \Big(\gamma \langle Y^3 \rangle^{1/2}\Big)\Big) \times \tanh\Big(\langle Y^3 \rangle^{1/2} \gamma/(2N\xi_1)\Big)\Big] \qquad (29)$$

where $\langle Y^3 \rangle = 1.6$.

Using Eqs. (19) and (29) for ξ_1 and ξ along with the contracted REs (3) and (4), we have calculated the average island density N and monomer density N_1 for both point and extended islands as a function of coverage as shown in Fig. 3. The starting coverage θ_0 for the integration was set to a small value ($\theta_0 \ll \theta_x$ with θ_x given by Eq. (22)) such that $N_1(\theta_0) \simeq \theta_0$ while the initial island density $N(\theta_0)$ was calculated using Eq. (21). As can be seen, this leads to excellent agreement with KMC simulations for both point and extended islands over the whole coverage range.

4. Gap evolution equations

4.1. Gap evolution equations for point islands

In order to obtain the coverage and size-dependent capture numbers $\sigma_s(\theta)$, one needs to go beyond MF theory and consider the dependence of the gap size on the cluster size s. We first consider the case of point islands and begin by defining $G_s(\theta; y)$ as the number of gaps of size y near clusters of size s at coverage θ. While a full set of gap-evolution equations including the effects of island growth, dimer nucleation, and the break-up of gaps by nucleation may be written [44], the resulting equations are quite complicated and difficult to solve. However, taking into account the generation of new gaps by the nucleation of dimers as well as the growth of islands by aggregation, and ignoring the break-up of gaps by nucleation, one can write a general set of evolution equations for the gap densities $G_s(\theta; y)$ in the following form,

$$\frac{\mathrm{d}G_2(\theta; y)}{\mathrm{d}\theta} = (\mathrm{d}N/\mathrm{d}\theta)\delta(y - \langle y \rangle) - RN_1\tilde{\sigma}(y)G_2(\theta; y) \qquad (30)$$

$$\frac{\mathrm{d}G_s(\theta; y)}{\mathrm{d}\theta} = RN_1\tilde{\sigma}(y)[G_{s-1}(\theta; y) - G_s(\theta; y)] \quad (s \geqslant 3) \qquad (31)$$

where $\tilde{\sigma}(y) = (2\xi_1/\gamma\xi^2)\tanh(y/2\xi_1)$. The first term on the right side of Eq. (30) corresponds to dimer nucleation, while the remaining terms in Eqs. (30) and (31) correspond to growth of islands via aggregation. Since we expect the average size of new gaps generated by nucleation to be equal to the average gap size $\langle y \rangle = \gamma/N$ at that coverage, for simplicity we have assumed in Eq. (30) that the size of new gaps generated by nucleation is exactly given by the average gap size $\langle y \rangle$. Rewriting the nucleation term in Eq. (30) as $B_y\delta(\theta - \theta_y)$, where θ_y is defined by the condition $y = \gamma/N(\theta_y)$, the dimer-gap evolution Eq. (30) may be rewritten

$$\frac{\mathrm{d}G_2(\theta; y)}{\mathrm{d}\theta} = B_y\delta(\theta - \theta_y) - RN_1\tilde{\sigma}(y)G_2(\theta; y) \qquad (32)$$

where $B_y = \gamma/y^2$.

As already noted, the gap-evolution equations (31) and (32) do not include terms corresponding to the "break-up" of existing gaps due to nucleation within a gap. While such terms can be added they render an analytic solution intractable. Instead we will solve Eqs. (31) and (32) and then account for the break-up of gaps due to nucleation by a uniform rescaling of the gap distribution.

The set of Eqs. (31) and (32) constitute a two-dimensional set of equations (in s and in y) which are quite difficult to solve directly numerically. However, by transforming to new variables,

$$x_y = \int_{\theta_y}^{\theta} RN_1(\theta')\tilde{\sigma}(y;\theta')\mathrm{d}\theta' \tag{33}$$

the gap equations (31) and (32) can be put in a form which can be solved analytically, i.e.

$$\frac{\mathrm{d}G_2(x_y;y)}{\mathrm{d}x_y} = -G_2(x_y;y) + B_y\delta(x_y) \tag{34}$$

$$\frac{\mathrm{d}G_s(x_y;y)}{\mathrm{d}x_y} = G_{s-1}(x_y;y) - G_s(x_y;y) \quad (s \geqslant 3) \tag{35}$$

The solution of Eq. (34) is $G_2(x_y;y) = B_y\mathrm{e}^{-x_y}H(x_y)$ where $H(z)$ is the step-function ($H(z) = 1,\ z \geqslant 0;\ H(z) = 0, z < 0$). In addition one may show (see Appendix A) that the general solution for the gap distribution for $s \geqslant 2$ is

$$G_s(y) = B_y x_y^{s-2}\,\mathrm{e}^{-x_y}/(s-2)! \tag{36}$$

For $\theta \ll \theta_x$ one may show (see Appendix B) that x_y is small and so the distribution $G_s(y)$ is relatively "flat" as a function of y. This corresponds to the MF result $y_s = \langle y\rangle$ as one expects in the nucleation regime. However, at late time, both x_y and the average gap size y_s are typically large and so Eq. (36) corresponds to a sharply peaked distribution as a function of y with a peak at $y = \hat{y}_s$. Neglecting the y-dependence of B_y (which is negligible compared to that due to the terms depending on x_y), one obtains for the peak $\hat{y}_s$ of the gap distribution

$$x_{\hat{y}_s} = s - 2 \tag{37}$$

We note that for dimers, Eq. (37) implies, using Eq. (33) and the definition of θ_y, $\hat{y}_2 = \gamma/N$ as expected.

Thus, neglecting the effects of break-up, the average length y_s of a gap near an island of size s, and the capture numbers σ_s will satisfy (keeping in the sums only the dominant term),

$$y_s \equiv \frac{\sum_y y\,G_s(x_y;y)}{\sum_y G_s(x_y;y)} = \hat{y}_s \tag{38}$$

$$\sigma_s \equiv \frac{\sum_y \tilde{\sigma}(y)G_s(x_y;y)}{\sum_y G_s(x_y;y)} = \tilde{\sigma}(\hat{y}_s) \tag{39}$$

As has already been noted, however, the gap equations (31) and (32) do not include the effects of the break-up of gaps due to nucleation. Therefore, the average gap sizes calculated using Eq. (37) are expected to be larger than the correct values. To include the effects of break-up, the gap lengths must be rescaled to give the correct average gap-length $\langle y\rangle = \gamma/N$. Thus, the correct capture numbers σ_s may be calculated using

$$\sigma_s = \tilde{\sigma}(y_s') \quad \text{where } y_s' = \frac{\gamma\hat{y}_s}{\sum_s N_s\hat{y}_s} \tag{40}$$

and where $\tilde{\sigma}(y) = (2\xi_1/\gamma\xi^2)\tanh(y/2\xi_1)$. Therefore, the calculation of the size-dependent capture numbers has been reduced to solving Eqs. (37) and (40) and the full REs (1) and (2) can be integrated to find the island-size distributions.

We now summarize how in practice Eqs. (37)–(40) are used to obtain the capture numbers in the course of our RE calculations. For any given s, Eq. (37) is solved numerically to find the solution $\hat{y}_s$ by calculating the integral x_y as given by Eq. (33) for different values of y. In calculating x_y for each value of y needed in the numerical routine (we have used Ridders' method), Eq. (9), along with Eqs. (19) and (29) for ξ_1 and ξ, is used for the local capture number $\tilde{\sigma}_s(y)$ which enters in Eq. (33). Once the solutions $\hat{y}_s$ have been calculated for all s, they are rescaled following Eq. (40) to obtain y_s'. As described in Eq. (40), y_s' is then used in Eq. (9) to obtain σ_s. We note that calculating x_y using Eq. (33) requires knowing $N_1(\phi)$ for all coverages ϕ up to the present coverage θ. While in principle, these values can be stored during the integration, for numerical convenience we have used the pre-calculated $N_1(\theta)$ obtained in Section 3.4.

4.2. Results for point islands

Using our gap-evolution equation results as described above, the full REs (1) and (2) were numerically integrated in order to obtain the scaled island-size distribution $f(s/S) = (S^2/\theta)N_s$ (where $S = (\theta - N_1)/N$ is the average island size) as a function of coverage for point islands. The REs were integrated starting at an initial coverage $\theta_0 \ll \theta_x$, with initial conditions $N_1(\theta_0) = \theta_0$, $N_2(\theta_0) = (4/5)R^{1/2}\theta^{5/2}$, and $N_s(\theta_0) = 0$ for $s \geqslant 3$ using the capture numbers σ_s as described above. At low

coverage, for which the island-size distribution is not sharply peaked and for which both the average island size and x_y are small, the island capture numbers σ_s were taken to be equal to the MF value $\sigma_{\rm av} = (\xi^{-2} - \xi_1^{-2})/N$ for all s. However, at higher coverages when the peak in the gap-distribution $G_s(y;\theta)$ is well-defined (we chose as criterion $S \geqslant 10$) the gap-evolution equation result (40) for σ_s was used. At each integration step, the variables x_y were updated over the range of relevant values of y and Eqs. (37) and (40) were then used to obtain the capture numbers σ_s.

Fig. 4 shows typical results for the calculated scaled island-size distributions for point islands in the aggregation regime ($\theta = 1.0$ and 3.0) for $D_{\rm h}/F = 10^7$ and 10^8 along with the corresponding KMC simulation results. As can be seen, there is excellent agreement between the predicted island-size distributions and the simulation results. In addition, the scaled distributions appear to show excellent scaling i.e. they depend only weakly on coverage. Also shown for comparison (dashed lines) are results obtained using the MF approximation $\sigma_s = \sigma_{\rm av}(\theta)$ which corresponds to the absence of a correlation between the island size and the capture number. As can be seen, the scaled MF distributions are much more sharply peaked with a peak height that increases rapidly with increasing coverage and appear to be approaching the asymptotic form [27] $f_{\rm MF}(s/S) = (1/4)(1 - s/S)^{-2/3}$. Such behavior is similar to the divergence predicted in Refs. [27,28,30,35] and is due to the lack of correlations between the island size s and the "capture zone" in the MF approximation. In addition, we note that the value of $f(0)$ obtained by both our simulations and our RE predictions is significantly above the MF prediction of $f_{\rm MF}(0) = 1/4$.

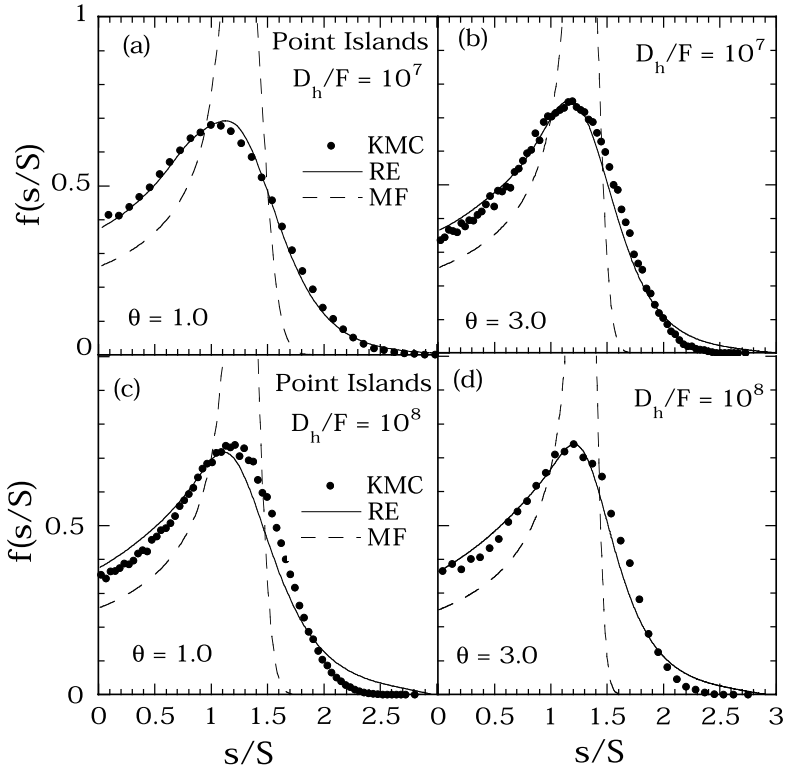

Fig. 4. Scaled island-size distribution $f(s/S) = (S^2/\theta)N_s(\theta)$ for point islands ($D_{\rm h}/F = 10^7$ and 10^8) calculated using gap evolution equations (solid lines) along with corresponding KMC results (symbols) at coverage $\theta = 1$ and 3. Dashed lines correspond to MF results.

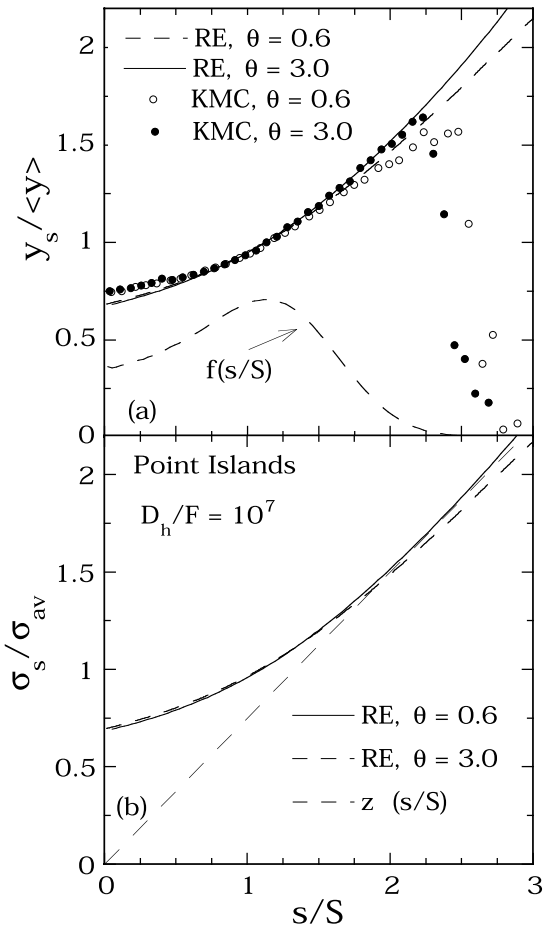

Fig. 5. (a) Scaled average gap size $y_s/\langle y\rangle$ and (b) capture-number distributions $\sigma_s/\sigma_{\rm av}$ for point islands for $D_{\rm h}/F = 10^7$ as a function of scaled island size for $\theta = 0.6$ and 3.0, obtained from gap evolution equations (RE) along with corresponding simulation results (KMC).

In order to understand the scaling behavior observed in our calculated island-size distributions, in Fig. 5(a) we have plotted the calculated scaled average gap-size $y_s/\langle y\rangle$ corresponding to an island of size s as a function of the scaled island-size s/S obtained from our gap-evolution equations for $\theta = 0.6$–3.0 and $D_{\rm h}/F = 10^7$ along with the corresponding results obtained from KMC simulations. As can be seen, there is good agreement between the scaled gap-size distribution predicted by our calculations and the simulations. Also shown in Fig. 5(a) is the scaled island-size distribution $f(s/S) = N_s(\theta)S^2/\theta$. As can be seen, the main discrepancy between the scaled gap-size distribution predicted by the gap-evolution equations and the simulation results occurs for $s/S > 2$ and is due to the absence of a cutoff (which should occur due to break-up) in the calculated distribution. However, this has little effect on the calculated capture numbers σ_s or on the resulting island-size distribution because the island density is extremely small over this range of island sizes.

Using Eq. (40) for the capture number $\sigma_s = \tilde{\sigma}(y_s')$, where y_s' is the average gap size corresponding to an island of size s, we can also calculate the scaled capture number $\sigma_s/\sigma_{\rm av}$ as a function of the scaled island size $u = s/S$ as shown in Fig. 5(b). For both $D_{\rm h}/F = 10^7$ and 10^8 (not shown), the scaled distribution is essentially independent of coverage and appears to be approaching the limiting form $\sigma_s/\sigma_{\rm av} = zu$ for large u where $z = 3/4$ [27] is the dynamical exponent corresponding to irreversible point-island growth in one dimension. This behavior is in agreement with that predicted and previously observed in Monte Carlo simulations by Bartelt and Evans [35].

4.3. Gap evolution equations for extended islands

We now consider the gap evolution equations for the case of extended islands. In this case, it turns out to be easier to consider a set of gap-evolution equations for the distribution of distances $\tilde{y}$ between the center of an island and the center of the nearest island. Assuming no correlation between the size of an island and the size of the nearest island, then the actual average gap distance y_s corresponding to an island of size s may be approximated as $y_s \simeq \tilde{y}_s - (s+S)/2$.

In this case the gap-evolution equations become,

$$\frac{{\rm d}G_2(\theta;\tilde{y})}{{\rm d}\theta} = -RN_1\tilde{\sigma}_2(\tilde{y})G_2(\theta;\tilde{y}) + B_{\tilde{y}}\delta(\theta - \theta_{\tilde{y}}) \tag{41}$$

$$\frac{{\rm d}G_s(\theta;\tilde{y})}{{\rm d}\theta} = RN_1[\tilde{\sigma}_{s-1}(\tilde{y})G_{s-1}(\theta;\tilde{y}) - \tilde{\sigma}_s(\tilde{y})G_s(\theta;\tilde{y})] \quad (s \geqslant 3) \tag{42}$$

where $\tilde{\sigma}_s(\tilde{y}) \equiv \tilde{\sigma}(\tilde{y} - s/2 - S/2)$ and $B_{\tilde{y}} = 1/\tilde{y}^2$, $\theta_{\tilde{y}}$ is defined by the condition $\tilde{y} = 1/N(\theta_{\tilde{y}})$, and the effects of direct impingement of atoms on islands have been neglected in the gap-evolution equations since they are negligible except at high coverage.

Unfortunately, these equations cannot be solved analytically due to the explicit s-dependence in $\tilde{\sigma}_s(\tilde{y})$. However, using the MF approximation $\tilde{\sigma}_s(\tilde{y}) \simeq \tilde{\sigma}_S(\tilde{y})$ (where $S = (\theta - N_1)/N$ is the average island size) leads to a set of gap-evolution equations which can be solved. We note that the use of such a MF approximation in the gap-evolution equations still retains the dominant effect i.e. that of the capture zone y. Furthermore, the correct expression for $\tilde{\sigma}_s(\tilde{y})$ is still retained in the island-density REs (1) and (2). Therefore, we expect this approximation to have only a weak effect on the final island-size distributions $N_s(\theta)$.

Transforming as before to new variables,

$$x_{\tilde{y}} = \int_{\theta_{\tilde{y}}}^{\theta} RN_1(\theta')\tilde{\sigma}_S(\theta';\tilde{y})\mathrm{d}\theta', \tag{43}$$

the resulting gap equations become

$$\frac{\mathrm{d}G_2(x_{\tilde{y}};\tilde{y})}{\mathrm{d}x_{\tilde{y}}} = -G_2(x_{\tilde{y}};\tilde{y}) + B_{\tilde{y}}\delta(x_{\tilde{y}}) \tag{44}$$

$$\frac{\mathrm{d}G_s(x_{\tilde{y}};\tilde{y})}{\mathrm{d}x_{\tilde{y}}} = G_{s-1}(x_{\tilde{y}};\tilde{y}) - G_s(x_{\tilde{y}};\tilde{y}) \quad (s \geqslant 3) \tag{45}$$

The solution is given by

$$G_s(\tilde{y}) = B_{\tilde{y}}x_{\tilde{y}}^{s-2}\mathrm{e}^{-x_{\tilde{y}}}/(s-2)! \tag{46}$$

while the peak of the center-to-center distribution $\tilde{y}_s$ for a given s corresponds to

$$x_{\tilde{y}_s} = s - 2 \tag{47}$$

To include the effects of break-up, the gap lengths must again be rescaled to give the correct average center-to-center distance $\langle\tilde{y}\rangle = 1/N$. If one considers the rescaling to apply directly to the center-to-center distances, then the coverage-dependent capture numbers σ_s may be calculated using

$$\sigma_s = \tilde{\sigma}(y'_s - s/2 - S/2) \quad \text{where } y'_s = \frac{\tilde{y}_s}{\sum_s N_s\tilde{y}_s} \tag{48}$$

Another possibility is to apply the rescaling due to break-up directly to the gaps y_s rather than to the center-to-center distances. In this case one obtains

$$\sigma_s = \tilde{\sigma}(f\tilde{y}_s - s/2 - S/2) \quad \text{where } f = \frac{\gamma}{\sum_s \tilde{y}_s N_s + \gamma - 1} \tag{49}$$

Therefore, the calculation of the coverage-dependent capture numbers σ_s for extended islands has been reduced to solving Eqs. (43) and (47) by following a similar numerical procedure as for point islands, and the full island-density REs (1) and (2) can be integrated to find the island-size distributions.

4.4. Results for extended islands

Fig. 6 shows our RE results (solid lines) obtained using the gap-evolution and island-density REs for the scaled island-size distribution for extended islands in the aggregation regime ($\theta = 0.3$ and 0.5, $D_h/F = 10^7$ and 10^8) along with the corresponding simulation results (symbols). As can be seen, there is good agreement between the calculated distributions and the KMC simulations. Also shown in Fig. 6 are the corresponding MF results (dashed lines) which lead to scaled island-size distributions which are much more sharply peaked and appear to diverge with increasing coverage and D_h/F.

In contrast to our point-island results, for extended islands $f(0)$ decreases with increasing coverage. The existence of a small value of $f(0)$ for irreversible growth of extended islands has been previously observed experimentally [13,14] for the case of two-dimensional submonolayer growth as well as in two-dimensional simulations [30]. Surprisingly, the value of $f(0)$ obtained from the MF calculations (dashed lines) which were obtained using coverage-dependent but not size-dependent capture numbers, agree relatively well with the gap-evolution and simulation values even though the rest of the distribution does not. This indicates that the decrease in $f(0)$ with increasing coverage is not due to coalescence, since coalescence is not taken into account in either the MF or gap-evolution

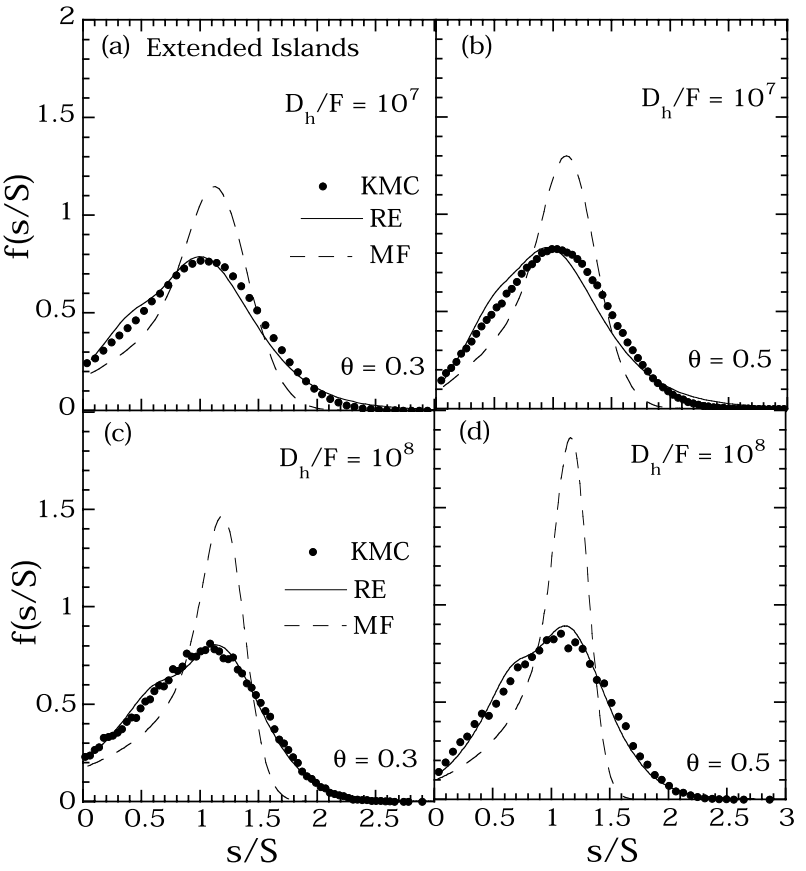

Fig. 6. Scaled island-size distribution $f(s/S) = (S^2/\theta)N_s(\theta)$ for extended islands ($D_h/F = 10^7$ and 10^8) calculated using gap evolution equations (solid lines) along with corresponding KMC results (symbols) at coverage $\theta = 0.3$ and 0.5. Dashed lines correspond to MF results.

equations, but is most likely due to the rapid increase in the average capture number σ_{av} with coverage for extended islands. The evolution of the scaled island-size distribution with coverage for small scaled island size is also an indication of incomplete scaling for extended islands [23].

Fig. 7 shows the corresponding results for the scaled average gap size $y_s/\langle y\rangle$ as a function of the scaled island size for $D_h/F = 10^8$ and $\theta = 0.3$ and 0.5. As for the point-island case, the main discrepancy between the calculated values of the average gap size y_s and simulation occurs for large scaled island size and is due to the absence of a cutoff in the calculated distribution. However, just as for the point-island case, this has a negligible effect on the calculated capture numbers or on the island-size distribution because the island density N_s is extremely small for large s/S.

Fig. 8 shows the corresponding RE results for the scaled capture number distribution $C(s/S) = \sigma_s/\sigma_{av}$ for extended islands for $D_h/F = 10^7$ and 10^8 and $\theta = 0.1$–0.5. In contrast to the point-island case, the scaled capture number distribution $C(u)$ is almost constant for $u < 1$ but increases rapidly for $u > 1$. For extended islands, the asymptotic dynamical exponent z_{ext} (where $S \simeq \theta/N \sim \theta^z$) is equal to 1, since one expects constant island density for $\theta_x \ll \theta < \theta_C$ where θ_C indicates the onset of island coalescence. This is in contrast to the point-island value $z_{pt} = 3/4$ in one dimension [27]. However, as can be seen from Fig. 3(b), for extended islands and $D_h/F = 10^7$–10^8, the regime of

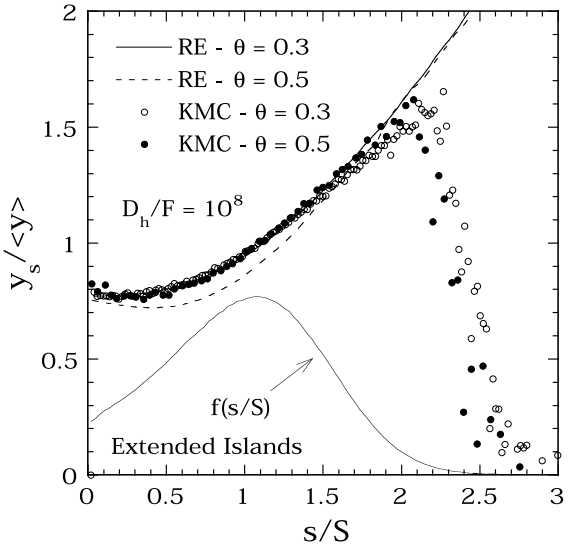

Fig. 7. Scaled average gap-size $y_s/\langle y\rangle$ for extended islands ($D_h/F = 10^8$) as a function of scaled island size for $\theta = 0.3$ and $\theta = 0.5$ obtained from gap-evolution equations (lines) along with corresponding simulation results (symbols).

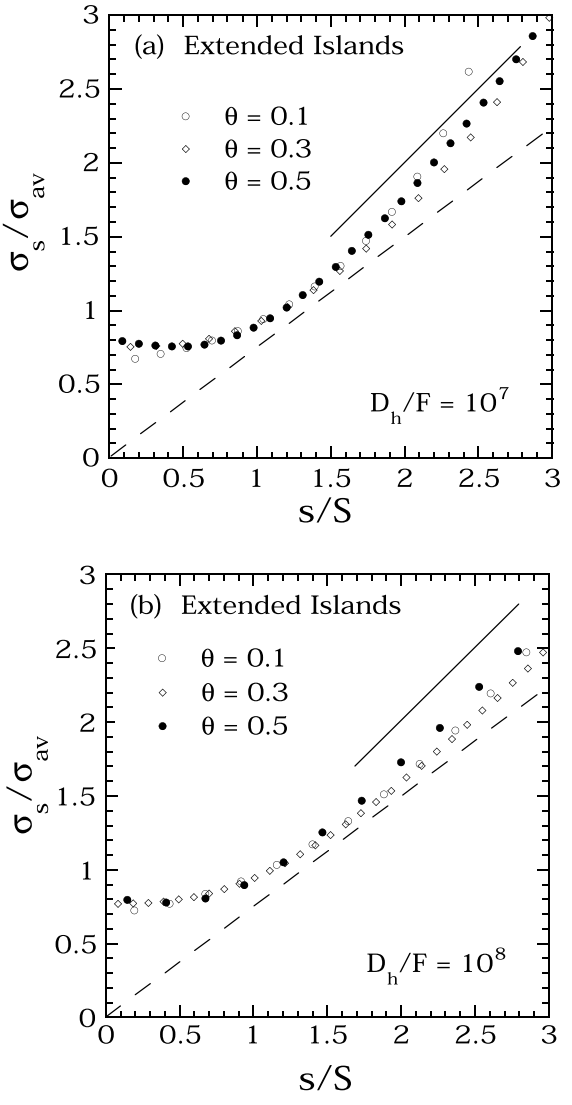

Fig. 8. Scaled capture-number distribution σ_s/σ_{av} for extended islands obtained from gap-evolution equations with (a) $D_h/F = 10^7$ and (b) $D_h/F = 10^8$. Solid lines correspond to theoretical asymptotic limit $C(u) = zu$ where $z = 1$. Dashed lines correspond to point-island limit $C(u) = (3/4)u$.

constant island density has just been reached at $\theta = 0.5$ and so the effective value of z is actually somewhere between the point-island value $z = 3/4$ and the asymptotic value $z = 1$. Therefore it is not surprising that the predicted scaled capture-number distribution $C(s/S)$ crosses the line $C(u) = u$ near $u = 1$. Similar behavior has been observed in Monte Carlo simulations of two-dimensional point-islands by Bartelt and Evans [35]. We note however, that the predicted capture number distributions remain clearly above the point-island asymptotic limit $C(u) = (3/4)u$. The approach of the slope of $C(u)$ to 1 for large u may also indicate a crossover to asymptotic extended-island scaling behavior.

5. Discussion

We have developed a self-consistent RE approach to irreversible submonolayer growth in one dimension which takes into account the existence of correlations between the size s of an island and the size of its "capture zone" or gap y_s and which consistently describes both point- and extended-island models. By solving the diffusion equation for the local monomer density within a gap self-consistently with the corresponding REs, we have obtained an explicit analytical expression for the

monomer capture number σ_1 which accurately predicts the rate of nucleation over the full range of coverage in the pre-coalescence regime. This expression indicates an unusual dependence of the capture number σ_1 on the monomer density N_1 and also correctly predicts the early time behavior of the island density N as well as the scaling behavior of the critical coverage θ_x corresponding to the end of the nucleation regime. By self-consistently solving for the "capture length" ξ and incorporating the fluctuations in the gap distribution via the third moment of the gap distribution as in Ref. [34] we have also been able to quantitatively predict the average island capture number $\sigma_{\rm av}$ along with the monomer density N_1 and island density N as a function of coverage for both point- and extended-islands on a one-dimensional substrate.

To obtain the island-size distribution, we have proposed a second set of MF equations describing the evolution of the size-dependent capture zones. This second system was solved in closed form, and the solution was used to explicitly derive the correct size- and coverage-dependent capture zones y_s and capture numbers $\sigma_s(\theta)$ for irreversible submonolayer growth in one dimension. The predicted average gap sizes y_s were found to be in very good agreement with KMC simulations and led to capture-numbers σ_s which exhibit a strong dependence on the island-size s especially for large s. Using this set of capture numbers along with the full set of island-density REs, we have been able to accurately predict the scaled island-size distribution in the pre-coalescence regime for both point and extended islands.

It is interesting to ask why our approach works even though the "break-up" of existing gaps due to nucleation (which favors the break-up of large gaps over small gaps) has been approximated by a uniform rescaling of the gaps obtained in the gap-evolution equations. In considering this question it is important to realize that there are actually two competing effects. While nucleation favors the formation of large gaps, it also favors the break-up of larger gaps so that in some sense the two effects cancel out, except for a rescaling factor. Therefore, by ignoring both of these effects in our gap-evolution equations such a rescaling approach may be used. In this connection we note that our assumption that the gap-size of a freshly nucleated dimer (before rescaling) is equal to the average already-existing gap size turns out to be crucial in obtaining reasonable results and is consistent with the neglect of *both* break-up effects in the gap-evolution equations. A more detailed explanation may also be provided by a study of the scaling properties of the joint distribution function $G_s(y)$.

We note that an important factor in the present approach was the simple geometry corresponding to one-dimensional growth. Nevertheless, in higher dimensions the idea of evolution of capture zones still applies, and we have developed an extension of the present approach to the important case of irreversible submonolayer growth in two dimensions [45]. It is also worth noting that the use of coupled evolution equations for the capture zones and island densities may also prove useful in the study of a variety of other problems including reversible submonolayer growth, heteroepitaxial growth, and Ostwald ripening.

Acknowledgements

This research was partially supported by the Office of Naval Research through grant number N00014-96-1-0536 to Emory University.

Appendix A. Solution of gap-evolution equations for $s \geqslant 3$

The rescaled gap equations (35) are

$$\mathrm{d}G_s(x_y;y)/\mathrm{d}x_y = G_{s-1}(x_y;y) - G_s(x_y;y) \quad (s \geqslant 3) \tag{A.1}$$

where $G_2(x_y;y) = B_y \mathrm{e}^{-x_y}$. Defining the generating function $g(x_y,u) = \sum_{s=2}^{\infty} G_s(x_y;y)u^{s-2}$ and substituting into Eq. (A.1) we obtain

$$\frac{\partial g(x_y,u)}{\partial x_y} = (u-1)g(x_y,u) \tag{A.2}$$

The solution of Eq. (A.2) consistent with $g(x_y,0) = G_2(x_y)$ is

$$g(x_y,u) = B_y \mathrm{e}^{(u-1)x_y} = B_y \mathrm{e}^{-x_y} \sum_{k=2}^{\infty} (ux_y)^{k-2}/(k-2)! \tag{A.3}$$

From Eq. (A.3) and the definition of $g(x_y, u)$, we obtain

$$G_s(x_y; y) = B_y x_y^{s-2} \mathrm{e}^{-x_y}/(s-2)!$$

Appendix B. Proof that $x_y \ll 1$ in nucleation regime

The definition of x_y (see Eq. (33)) is

$$x_y = \int_{\theta_y}^{\theta} \mathrm{d}\theta' R N_1(\theta') \tilde{\sigma}(y; \theta') \tag{B.1}$$

where $\tilde{\sigma}(y; \theta') = (2\xi_1/(\gamma\xi^2))\tanh(y/(2\xi_1))$. In the nucleation regime corresponding to $\theta \ll \theta_x$ the island density $N = \gamma/y$ is much less than the monomer density N_1. This implies that for typical values of y one has $y \gg \xi_1$ and one may approximate $\tanh(y/(2\xi_1)) \simeq 1$ in Eq. (B.1). In the nucleation regime one also has, $N_1 \simeq \theta$ and $\xi_1 \simeq \xi$. Using these along with Eq. (19) for ξ_1 and ignoring factors of order 1 leads to

$$x_y \simeq R^{3/4}(\theta^{9/4} - \theta_y^{9/4}) \tag{B.2}$$

However, in the nucleation regime one has $\theta \ll \theta_x \sim R^{-1/3}$. This implies that in the nucleation regime $x_y \ll 1$.

References

[1] J.Y. Tsao, Materials Fundamentals of Molecular Beam Epitaxy, World Scientific, Singapore, 1993.
[2] Y.W. Mo, J. Kleiner, M.B. Webb, M.G. Lagally, Phys. Rev. Lett. 66 (1991) 1998.
[3] H.J. Ernst, F. Fabre, J. Lapujoulade, Phys. Rev. B 46 (1992) 1929.
[4] R.Q. Hwang, J. Schroder, C. Gunther, R.J. Behm, Phys. Rev. Lett. 67 (1991) 3279.
[5] R.Q. Hwang, R.J. Behm, J. Vac. Sci. Technol. B 10 (1992) 256.
[6] W. Li, G. Vidali, O. Biham, Phys. Rev. B 48 (1993) 8336.
[7] E. Kopatzki, S. Gunther, W. Nichtl-Pecher, R.J. Behm, Surf. Sci. 284 (1993) 154.
[8] G. Rosenfeld, R. Servaty, C. Teichert, B. Poelsema, G. Comsa, Phys. Rev. Lett. 71 (1993) 895.
[9] J.-K. Zuo, J.F. Wendelken, Phys. Rev. Lett. 66 (1991) 2227.
[10] J.-K. Zuo, J.F. Wendelken, H. Durr, C.-L. Liu, Phys. Rev. Lett. 72 (1994) 3064.
[11] D.D. Chambliss, R.J. Wilson, J. Vac. Sci. Technol. B 9 (1991) 928.
[12] D.D. Chambliss, K.E. Johnson, Phys. Rev. B 50 (1994) 5012.
[13] J.A. Stroscio, D.T. Pierce, R.A. Dragoset, Phys. Rev. Lett. 70 (1993) 3615.
[14] J.A. Stroscio, D.T. Pierce, Phys. Rev. B 49 (1994) 8522.
[15] Q. Jiang, G.C. Wang, Surf. Sci. 324 (1995) 357.
[16] F. Tsui, J. Wellman, C. Uher, R. Clarke, Phys. Rev. Lett. 76 (1996) 3164.
[17] J.A. Venables, G.D. Spiller, M. Hanbucken, Rep. Prog. Phys. 47 (1984) 399.
[18] J.A. Venables, Philos. Mag. 27 (1973) 697.
[19] J.A. Venables, Phys. Rev. B 36 (1987) 4153.
[20] J.A. Blackman, A. Wilding, Europhys. Lett. 16 (1991) 115.
[21] F. Family, P. Meakin, Phys. Rev. Lett. 61 (1988) 428.
[22] C. Ratsch, A. Zangwill, P. Smilauer, D.D. Vvedensky, Phys. Rev. Lett. 72 (1994) 3194.
[23] J.G. Amar, F. Family, P.M. Lam, Phys. Rev. B 50 (1994) 8781.
[24] A.D. Gates, J.L. Robins, Surf. Sci. 116 (1982) 188.
[25] A.D. Gates, J.L. Robins, Surf. Sci. 191 (1987) 492.
[26] A.D. Gates, J.L. Robins, Surf. Sci. 191 (1987) 499.
[27] M.C. Bartelt, J.W. Evans, Phys. Rev. B 46 (1992) 12675.
[28] M.C. Bartelt, J.W. Evans, J. Vac. Sci. Technol. A 12 (1994) 1800.
[29] G.S. Bales, D.C. Chrzan, Phys. Rev. B 50 (1994) 6057.
[30] J.G. Amar, F. Family, Phys. Rev. Lett. 74 (1995) 2066.
[31] P.A. Mulheran, J.A. Blackman, Philos. Mag. Lett. 72 (1995) 55.
[32] M.C. Bartelt, J.W. Evans, Surf. Sci. 344 (1995) 1193.
[33] J.G. Amar, F. Family, Thin Solid Films 272 (1996) 208.
[34] J.A. Blackman, P.A. Mulheran, Phys. Rev. B 54 (1996) 11681.
[35] M.C. Bartelt, J.W. Evans, Phys. Rev. B 54 (1996) R17359.
[36] P.A. Mulheran, J.A. Blackman, Surf. Sci. 376 (1997) 403.
[37] T.R. Linderoth, S. Horch, E. Lægsgaard, I. Stensgaard, F. Besenbacher, Phys. Rev. Lett. 78 (1997) 4978.
[38] G.S. Bales, A. Zangwill, Phys. Rev. B 55 (1997) 1973.
[39] H. Kallabis, P.L. Krapivsky, D.E. Wolf, Eur. Phys. J. B 5 (1998) 801.
[40] M.N. Popescu, J.G. Amar, F. Family, Phys. Rev. B 58 (1998) 1613.
[41] M.C. Bartelt, A.K. Schmid, J.W. Evans, R.Q. Hwang, Phys. Rev. Lett. 81 (1998) 1901.
[42] M. von Smoluchowski, Z. Phys. Chem. 17 (1916) 557.
[43] S.M. von Smoluchowski, Z. Phys. Chem. 92 (1917) 129.
[44] J.G. Amar, M.N. Popescu, F. Family, Phys. Rev. Lett. 86 (2001) 3092.
[45] M.N. Popescu, J.G. Amar, F. Family, unpublished.